ACADEMIC PRESS

Available online at www.sciencedirect.com
SCIENCE DIRECT®

Journal of Catalysis 218 (2003) 12–23

JOURNAL OF CATALYSIS

www.elsevier.com/locate/jcat

Study of *n*-octane hydrocracking and hydroisomerization over Pt/HY zeolites using the reactors of different configurations

Peter N. Kuznetsov

Institute of Chemistry and Chemical Technology, Siberian Branch of Russian Academy of Sciences, K. Marx 42, Krasnoyarsk 660049, Russia

Received 9 July 2002; revised 25 February 2003; accepted 17 March 2003

Abstract

The conversion of *n*-octane over a series of monofunctional HY zeolites, which differed with the contents of Na and over the bifunctional Pt/HY zeolites differed with the contents of Pt, was studied as function of the balance among the specific activity of the components, the distribution of the metallic sites over zeolite surfaces and reaction conditions. The activities of individual metal and zeolite components were quantified in the reactions of 1-hexene hydrogenation and *n*-octane cracking, respectively. Gradientless reactors of different configurations were applied to rationalize the contribution of hydrogenation, dehydrogenation, cracking, isomerization, oligomerization, and catalyst deactivation reactions to the reaction pathways over the bifunctional Pt/HY zeolites. The conceptual bifunctional mechanism involving the dehydrogenation of *n*-octane into olefinic counterparts was demonstrated experimentally by using the flow circulation unit equipped with two reactors connected in series and loaded with separated HY and Pt components. The limiting steps were determined depending on the activity of the Pt component in Pt/HY. It was shown that an optimum concentration of Pt sites exists in HY zeolites which corresponds to a maximum cracking activity followed by a significant decrease as the concentration of metallic sites further increases. The effect of diffusion transfer of branched octene intermediates inside the zeolite cavities from the acidic sites to Pt sites on the rates and reaction pathways over Pt/HY zeolites is argued.

Keywords: Hydrocracking; Hydroisomerization; Bifunctional catalysts; Zeolite; Olefin; Diffusion

1. Introduction

Hydrocracking and hydroisomerization of hydrocarbons are the basic processes in the petroleum refining industry which produce a broad range of highly valuable chemicals, diesel oil, petrol, and gasoline. They proceed over bifunctional catalysts with two quite different components representing metallic and acidic functions. Different zeolites and zeolite-like solid acids and also acidic oxides are used as the acidic components. Decationized Y and mordenite zeolites are the most widely applied. This is mainly due to strong acidic properties combined with the specific pore geometry of these molecular sieves [1–6]. On the other hand, different metals such as Pt, Pd, Ni, Co, Mo, their oxides, and sulfides serve as the hydrogenating/dehydrogenating components. Metallic platinum is the most active catalyst and as few as 0.2–0.5 wt% are required to promote the activity of bifunctional contact.

According to the classic mechanism [7], the skeletal isomerization and hydrocracking of alkanes over bifunctional catalysts occur through a set of parallel and consecutive steps involving dehydrogenation of the alkane molecule over the metallic site to produce the respective olefin which is highly reactive for carbenium ion conversion and rapidly isomerizes and/or cracks into two smaller olefins over the acidic sites. The cracked and isomerized olefinic intermediates are hydrogenated at the final step. However, there is evidence [8–11] that the rate of the alkane hydrocracking and isomerization is dependent on the activity of metallic function. For example, the alkane hydroconversion over the catalysts with a high concentration of metallic components was significantly lower than that with less concentration [8,10]. The drop in the *n*-hexane isomerization activity was observed [10] when the contents of Pt and Ni in the HY zeolite exceeded their optimum levels of 0.6 and 3.0%, respectively. The authors [11] reported that even though monofunctional H-mordenite deactivated during *n*-butane isomerization, it still had a better activity after 60 min on stream than the

E-mail address: kuzpn@krsk.info.

0021-9517/03/$ – see front matter
doi:10.1016/S0021-9517(03)00139-8

Pt-loaded HM mordenite. This is difficult to explain in terms of a traditional kinetic chemical network.

The alternative bifunctional concept suggests that the initial activity of acidic components with strong acidity is high enough to activate an alkane molecule [12]. The main problem associated with the use of strongly acidic catalysts is the fast deactivation by carbonaceous species generated from the olefinic precursors. The key role of metallic component in this bifunctional concept is to prevent poisoning and to maintain the performance of acid centers by means of hydrogen activation to hydrogenate the olefinic intermediates. For example, over the monofunctional H-mordenite, the high catalytic activity for *n*-butane isomerization decreased drastically with time on stream [11]. Deactivation was minimized by hydrogen and Pt loading that was thought to reduce the concentration of intermediate olefins in the zeolite pores. This concept raises some fundamental questions as to the nature of the zeolite-catalyzed reactions responsible for the initial activation of alkane molecule at rather low temperatures.

As to the acidic function of zeolites two main pathways of the alkane conversion are currently discussed [1,2,4,13–15]: (i) a bimolecular carbenium ion mechanism involving the activation of the alkane molecule via hydride transfer to a carbenium ion followed by β-scission of this newly formed carbenium ion, (ii) a monomolecular pathway of direct activation of alkane molecules. The generation of carbenium ions in a bimolecular reaction is normally associated with the sorption of olefins on the Brønsted acid sites. Note that chemosorbed alkenes are currently accepted [2,13,16–20] to exist as alkoxy groups which on excitation form the carbenium ions in the transition state. Carbonium ion is believed to represent rather a transition state than a stable, high-energy intermediate. However, the structure of the reactive intermediates is not specified in this paper.

The beneficial effect of olefin additives on the cracking and isomerization of alkanes over zeolites has been demonstrated by many authors [13,21–28]. According to recent evidence obtained by Dumesic and co-workers [22,23], the isomerization of isobutane over the H-mordenite and USY zeolites at low temperatures did not commence without the presence of traces of olefins in the feed. The addition of olefins (isobutylene) dramatically increased the rate of isomerization as well as the rates of side reactions such as oligomerization/β-scission and coking resulting in catalyst deactivation.

A dual contrasting function of olefins in the zeolite-catalyzed reactions makes it difficult to discriminate between the monomolecular and bimolecular pathways. The detection of the monomolecular reaction is hindered usually by the bimolecular products which tend to dominate as conversion increases. Therefore, a solely monomolecular pathway in the reaction of alkane isomerization was observed only when the conversion was very low, less than 0.4–1.4% after Dumesic and co-workers [22], because spontaneous transition to the bimolecular reaction occurred as the amount of olefin products accumulated [22,29–33]. In our earlier papers [26–28], a gradientless flow circulation unit equipped with two reactors connected in series was applied to study the effect of olefinic products on the *n*-octane cracking over HY zeolites. First the reactor was loaded with HY zeolite for cracking and another one was loaded with 0.5% Pt/Al_2O_3 at 150 °C for hydrogenation of olefinic intermediates. Solely monomolecular cracking of even *n*-octane was found to take place in the reactor unit of this configuration to a high extent of conversion (up to 53%) due to controlled termination of the chain reaction as a result of olefin hydrogenation.

Also, evidence [8,9,34–40] was obtained that alkane conversion can be governed by the pore structure of the zeolite that distorted the kinetic data. For instance, hexane hydroisomerization rate was reported [34] to increase significantly after acid leaching of Pt/mordenite. The alleviation of intracrystalline diffusion limitation but not the alteration of acid centers was argued to be the major factor in activity enhancement. Although HY zeolite has wider pores compared to other zeolites, nevertheless diffusion transfer inside the pores is supposed [8,9,32,38,41–43] to affect fast chemical reactions of highly reactive olefins over both the metallic and the acidic sites.

The catalytic activity of metal-containing HY zeolites loaded with different amounts of Ni, Pd, and Pt in the reaction of *n*-octane hydrocracking has been studied earlier in our papers [27,44]. In terms of a classic bifunctional model [7], it should be expected that where the dehydrogenation function is limiting, the rate of *n*-octane hydrocracking must be identical at the same dehydrogenation rate whatever the metal's nature. Nevertheless, the hydrocracking rates proved to be quite different and increased in the order PtHY $\leqslant$ PdHY $<$ NiHY. The difference between the activities of bifunctional catalysts based on the same HY zeolite and having the same hydrogenating-dehydrogenating activity was difficult to explain, and further kinetic experiments are required to rationalize this anomaly.

A large volume of studies on *n*-alkane conversion over bifunctional metal-zeolite catalysts has been published in the literature; however, the reaction mechanism is very complicated and still not completely understood. It should be noted that detailed experimental evaluation of the kinetic parameters is problematic for rapidly deactivating zeolites especially when long-chain alkanes with enhanced reactivity are processed. This is the reason why the fundamental kinetic data on the hydrocracking and isomerization reactions were obtained largely with low molecular alkanes, *n*-butane and isobutane particularly [3,11, 22,23,32,45,46]. However, C_4–C_6 alkane molecules are too small to be representative of the alkanes of an industrial hydrocracking feed. Therefore the catalytic activity of bifunctional zeolite catalysts must be confirmed for longer alkanes. Also, because of zeolite deactivation es-

pecially when long-chain alkanes with enhanced reactivity are processed novel kinetic approaches are needed and extensive studies remain to be carried out before firm conclusions can be drawn as to the appropriate pathway of zeolite-catalyzed reactions and the true role of olefin intermediates.

In the present paper, the hydroconversion of *n*-alkane over the bifunctional Pt/HY zeolite catalysts is studied to better understand the roles of olefinic intermediates produced from dehydrogenation of the parent alkane molecule and that produced from its zeolite-catalyzed cracking. Reactors of different configurations were applied to control the concentration of olefinic intermediates and to avoid the problems related to deactivation. *n*-Octane was used as a reaction feed because it is the representative molecule of the alkanes of an industrial hydroisomerization and hydrocracking feeds and also all the possible modes of cracking and isomerization of carbenium ions can be involved during the hydroconversion reactions.

In the reactors that were conventionally applied in the kinetic evaluations, both hydrogenation-dehydrogenation and cracking-isomerization occurred simultaneously over the different components of bifunctional catalysts. This presents difficulties in the differentiation between the contributions of the reactions occurring on the metallic and zeolite sites to the total conversion, specific roles of *n*-alkane dehydrogenation, and that of hydrogenation of the cracked olefinic products, in particular. Also, experimental evaluation of the catalytic activity is problematic usually for rapidly deactivating zeolite catalysts. Therefore, the nongradient reactors (continuous-flow-circulation reactor and a microreactor) of different configurations were applied. The microreactor unit could operate both in a continuous-flow mode and in a pulse mode. The latter made it possible to evaluate the catalytic activity at the initial reaction period for the catalysts whose activity rapidly decreased. A continuous-flow-circulation unit equipped with two reactors connected in series allowed the metal and zeolite components to be separated and loaded in the different reactors at different temperatures. In this unit, the rates of hydrogenation, dehydrogenation, cracking, and isomerization were controlled independently and the effects of olefinic intermediates produced from *n*-octane dehydrogenation and from cracking were monitored.

Sets of HY and Pt/HY zeolites with a large variation in the activities of the components were used to better understand the bifunctional kinetic network. The catalytic activities of the individual metallic and zeolitic components in the specific reactions of 1-hexene hydrogenation and *n*-octane and 1-octene cracking were evaluated quantitatively. From the product distribution established on these quantitatively characterized catalysts with a large variation in the activity of components, the sequence of the various reaction steps during *n*-octane hydrocracking and isomerization was specified.

2. Experimental

HY zeolites with different quantities of Na were prepared according to [28] by repeated treatment of a commercial NaY zeolite with 0.1 N solution of $NH_4C1 + NH_4OH$ followed by calcination (between treatments) at 400 °C for 3 h. The HY zeolites produced were repeatedly treated with $[Pt(NH_3)_4]Cl_2$ solutions to prepare a set of Pt/HY samples with different Pt concentrations from 0.02 to 10.3 wt%. To produce fine metallic particles, Pt-loaded zeolites were treated at 350 °C in a dry air flow and then reduced by hydrogen in the catalytic reactor at 350 °C for 2 h before the catalytic tests [47].

The dispersion of Pt particles was studied by TEM. The crystallinity of the zeolite framework was controlled by X-ray diffraction and by argon desorption. The relative degree of crystallinity was estimated as the ratio of a sum of the integral intensities of (111), (220), (311), (331), (440), (533), and (642) reflexes to that of the original zeolite rated by 100%.

Specific catalytic activity of the metallic function was evaluated in the reaction of 1-hexene hydrogenation at 150 °C at atmospheric pressure, and quantified by the first-order rate constant [47]. To evaluate the specific monofunctional acidic function, HY zeolites with no Pt were tested in the reactions of *n*-octane, and 1-octene cracking. Bifunctional hydrocracking/isomerization activity of Pt/HY catalysts was evaluated in the reaction of *n*-octane hydroconversion.

Catalytic measurements were carried out in the reactors of different configurations under concentration and temperature gradientless conditions. A continuous-flow-circulation reactor unit (CFCR) and a microreactor unit (2-ml reactor volume) with a vibro-fluidized catalyst bed were used. The microreactor unit could operate both in a continuous-flow mode (CFMR configuration) and in a pulse mode (PMR configuration). The PMR configuration was used to evaluate the catalysts whose activity rapidly decreased. A mixture of *n*-octane (1 or 6 vol%) in H_2 (or in N_2) was used as a feed. In the microreactor of CFMR configuration, the feed entered the reactor continuously, and in the microreactor of PMR configuration, feed pulses (volume of 30 ml) were introduced periodically (via a multipass tap) into the continuous flow of H_2 (or N_2) through the reactor. Flow rate was so adjusted to vary pulse duration from 10 to 50 s. So, the PMR reactor had a short-reaction cycle, and made it possible to evaluate catalytic activity at the initial period.

In a continuous-flow-circulation reactor unit, CFCR, the circulation of the reaction mixture through the reactor was accomplished by a piston electromagnetic pump joined to a valve system allowing for one-directional flow in the reaction circuit. The rate of circulation was 600 $L\,h^{-1}$ and that of feeding the unit and of withdrawal of products was much less, 5–10 $L\,h^{-1}$. Due to a high circulation factor, the extent of *n*-octane conversion for a single circulation cycle was quite low (no more than 0.5%) making for concentra-

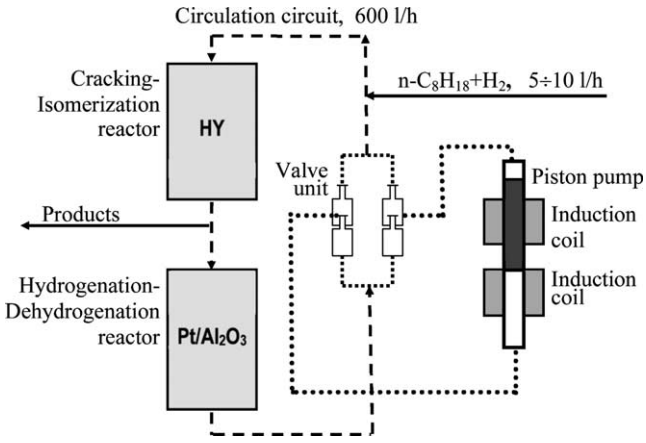

Fig. 1. Diagram of the continuous-flow-circulation unit with two reactors, CFCR of CR-HR configuration.

tion gradientless conditions. However, the cumulative extent of conversion varied in a broad range depending on the contact time (the ratio of the volume of catalysts to the rate of feeding) due to repeated circulation.

A CFCR equipped with an additional reactor connected in series (CR-HR configuration) was also applied. This catalytic unit allowed the metal and zeolite components to be separated and to be loaded in different reactors at different temperatures and the effect of olefinic intermediates which were produced from *n*-octane dehydrogenation and that of olefinic cracked products on the *n*-octane hydroconversion to be monitored. The schematic diagram of this unit is shown in Fig. 1. One of the reactors was loaded with HY zeolite for cracking/isomerization (CR reactor) and another one was loaded with 0.5% Pt/Al_2O_3 for hydrogenation/dehydrogenation (HR reactor). The temperature of each reactor was maintained separately. The products generated in CR were transferred into HR where unsaturated hydrocarbons were hydrogenated into the respective alkanes, and *n*-octane was dehydrogenated (when the temperature was high) into respective linear octenes over the 0.5% Pt/Al_2O_3 catalyst. This CFCR unit with CR-HR configuration made it possible to control the rates of hydrogenation/dehydrogenation and cracking/isomerization independently. The quantity of 0.5% Pt/Al_2O_3 in HR was so adjusted in the preliminary experiments to fully hydrogenate the olefinic intermediates but not to facilitate significantly other reactions, hydrogenolysis in particular.

The grain fraction 0.25–0.50 mm of the catalysts was used for catalytic measurements. Catalytic activity for *n*-octane conversion was quantified by the reaction rate normalized to the *n*-octane concentration in the reaction mixture ($W/[C_8H_{18}]$). The yield of C_3–C_5 hydrocarbons was considered to be a diagnostic regarding the acid-catalyzed cracking. C_1–C_2 hydrocarbon yield characterized mainly the activity for hydrogenolysis, and C_6–C_7 hydrocarbons were referred mainly to oligomerization-cracking reactions. The activity for hydroisomerization was determined from the total yield of branched C_8-hydrocarbons.

The reaction products were analyzed by gas chromatography using a column of 2.3 m in length filled with AW Hesasorb with polyphenyl ether at 120 °C and a column of 3.2 m in length filled with TZK with white paraffin oil at 65 °C.

3. Results

3.1. Specific characterization of HY zeolites

The characterization of prepared zeolites with 2.2, 1.7, and 0.9 wt% of Na contents is shown in Table 1. The evaluation of specific catalytic activity of HY zeolites for *n*-octane cracking was made under the conditions of monomolecular reactions in a CFCR unit with a CR-HR configuration at a temperature of 350 °C in CR and 150 °C in HR, and, according to [27,28], the first-order rate constants were calculated. It should be emphasized that HY zeolites showed quite stable operation under these conditions over a long period of time (up to 10 h), and no carbonaceous matter on the zeolite surface was formed. Reaction rate constants were found to increase dramatically as the content of Na decreased. HY0.9 was thus 2.5 times as active as HY1.7 and 18 times as active as HY2.2.

In continuously operated reactors of CFCR and CFMR configurations, the activity of zeolites in *n*-octane cracking was much higher, but decreased rapidly with time on stream due to olefin-assisted deposition of carbonaceous matter.

Shown in Table 2 are the data on the catalytic activity of the most active HY0.9 zeolite for the *n*-octane and 1-octene cracking evaluated in the microreactor of PMR configuration (pulse mode) at 350 °C. In the *n*-octane cracking, the zeolite did not undergo measurable deactivation when passing 5–10 pulses of feed, and the deactivation in 1-octene conversion was observed as the number of pulses increased. The average conversion of *n*-octane (for 5 pulses) was 39.6%, and complete conversion of 1-octene was observed in the first pulse. Hence, 1-octene reactivity for cracking evaluated as the normalized rate was more than about 10^3 times as active as *n*-octane. Mainly cracked C_3–C_5 hydrocarbons were produced from both molecules. However, the conversion of 1-octene also yielded C_6–C_7 hydrocarbons (13.5%) resulting from the oligomerization/β-cracking reactions.

Table 1
Characterization of HY zeolites

Zeolite	Content of Na (% wt)	SiO_2/Al_2O_3 ratio	Degree of crystallinity (%)	Cracking rate constant[a] ($L\,g^{-1}\,h^{-1}$)
HY2.2	2.2	4.0	100	0.10
HY1.7	1.7	4.0	100	0.25
HY0.9	0.9	5.0	70	1.80

[a] Continuous-flow-circulation reactor unit of CR-HR configuration, 350 °C in CR, 150 °C in HR, 0.18 MPa, hydrogen:*n*-octane molar ratio = 100.

Table 2
Conversion of *n*-octane and 1-octene over HY0.9 zeolite

Hydrocarbon	*n*-Octane	1-Octene
Feeding rate, h^{-1}	3.0	18.4
Conversion, %	39.5	100.0
W/C_8H_{18}, $L\,g^{-1}\,h^{-1}$	39.6	$> 4 \times 10^4$
Product composition, mol%		
Methane	–	–
Ethane, ethylene	0.8	0.6
Propane	17.2	3.5
Propylene	8.5	19.6
i-Butane	41.0	16.0
n-Butane	9.5	0.4
Butenes	6.7	29.3
i-Pentane	12.7	6.9
n-Pentane	2.6	0.2
Pentenes	1.0	10.4
Hexane–hexenes	–	3.8
Heptane–heptenes	–	9.7
Paraffin/olefin molar ratio	4.6	0.5
Iso/norm molar ratio	3.8	3.1

Pulse microreactor, 350 °C, 0.18 MPa, hydrogen:*n*-octane (1-octene) molar ratio = 100.

3.2. Specific characterization of Pt component of Pt/HY zeolites

Eight samples of Pt/HY0.9 catalysts with a PT content between 0.02 and 10.3% were prepared based on the most active HY0.9 zeolite with 0.9 wt% Na (Table 3). TEM study showed all Pt/HY0.9 catalysts to have a very homogeneous distribution of fine metallic particles which may be mainly located in the zeolite pores [6,32]. Displayed in Table 3 are the data on the catalytic activity of samples for the specific reaction of 1-hexene hydrogenation in a CFCR at 150 °C. The first-order rate constant referred to the amount of Pt/HY0.9 catalyst increased by two order of magnitude (from 180 to 16,500 $L\,g^{-1}\,h^{-1}$) as the content of Pt increased from 0.02 to 10.3 wt%. Using the specific activity of the unity of metallic surface of Pt for the same 1-hexene hydrogenation reaction [6,47], the surface area of Pt in Pt/HY zeolites and the ratios of the specific surface area of zeolite component to the specific surface area of metallic component depending on the content of Pt were estimated from the 1-hexene hydrogenation rate constants. One can see from Table 3 that Pt/HY0.9 samples represented a large possible variation of the activity of metallic components and their distribution over the zeolite surface.

Table 3
Characterization of metallic component of the Pt/HY0.9 zeolites and catalytic activity for 1-hexene hydrogenation at 150 °C

Catalyst	Pt content (wt%)	Rate constant, k_h ($L\,g^{-1}\,h^{-1}$)	Surface area of Pt[a] (m^2/g of Pt/HY)	S_{zeol}/S_{Pt} ratio[b]
HY0.9	No	–	–	–
0.02Pt/HY0.9	0.02	180	0.07	7860
0.06Pt/HY0.9	0.06	607	0.25	2200
0.2Pt/HY0.9	0.2	1600	0.66	833
0.5Pt/HY0.9	0.5	3643	1.5[d]	367
1Pt/HY0.9	1.0	7900	3.25	169
2Pt/HY0.9	2.3	10,000	4.12	133
8Pt/HY0.9	8.7	13,100	5.39	102
10Pt/HY0.9	10.3	16,500	6.79	81

Continuous-flow-circulation unit, 0.1 MPa, 1 $mmol^{-1}$ L of l-hexene in H_2.

[a] Surface area of metallic Pt in Pt/HY0.9 zeolites was calculated from the hydrogenation rate constants taking into account the data [6,47] on the surface area of Pt in 0.5Pt/HY0.9 sample (300 $m^2\,g^{-1}$ of Pt).

[b] The ratio of the surface area of zeolite (550 $m^2\,g^{-1}$) to the surface area of metallic Pt in Pt/HY0.9.

3.3. Bifunctional activity of Pt/HY0.9 zeolites in the reaction of *n*-octane hydroconversion

Shown in Fig. 2 is the catalytic activity of PtHY0.9 catalysts for *n*-octane conversion, cracking to C_3–C_5 hydrocarbons, and skeletal isomerization to branched octanes quantified by the normalized reaction rates plotted as a function of the specific hydrogenating activity quantified by the rate constant for 1-hexene hydrogenation, k_h. A continuous-flow-circulation unit with a single reactor (CFCR configuration) was used in these catalytic measurements. Deactivation of PtHY0.9 catalysts with poor hydrogenating activity was observed to some extent during the initial reaction period. In Fig. 2, the normalized reaction rates were referred to 30 min reaction time when a quasi-state reaction regime was attained, and the extent of conversion was adjusted within rather narrow limits (between 35 and 45%) by varying contact time. One can see from Fig. 2 that the total activity first increases proportionally to k_h and then attains a constant value over the catalysts with $\lg k_h \geqslant 3.5$. The rate of *n*-octane isomerization increases permanently in a non-monotonic manner, and the rate of cracking to C_3–C_5 hydrocarbons attains a maximum at $\lg k_h = 3.6$–3.9 and then decreases significantly as k_h further increases. The concentration of olefinic cracked products in the reaction mixture

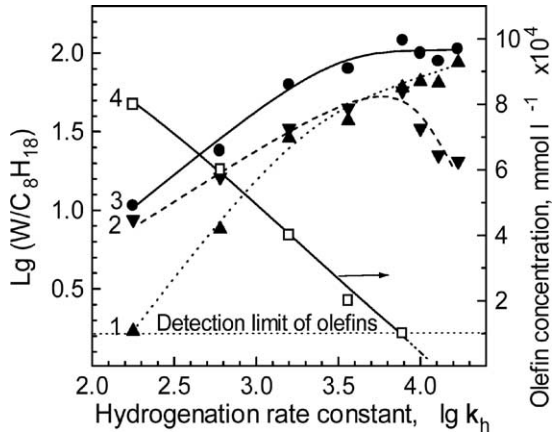

Fig. 2. The activity of Pt/HY0.9 catalysts in the *n*-octane hydroconversion in a flow circulation unit as a function of the hydrogenating activity of the platinum component. Flowcirculation unit, 300 °C, 0.18 MPa, H_2/C_8H_{18} molar ratio = 16. 1, Hydroisomerization; 2, cracking; 3, total *n*-octane conversion; 4, olefinic cracked product concentration.

Table 4
Selectivity of *n*-octane hydroconversion over different bifunctional Pt/HY0.9 catalysts

Catalyst	Selectivity (%)			C_3/C_5
	Cracking	Hydrogenolysis	Hydroisomerization	molar ratio
0.02Pt/HY0.9	82.2	1.8	16.0	1.10
0.06Pt/HY0.9	66.9	1.2	31.8	1.06
0.2Pt/HY0.9	53.6	0.4	46.0	0.98
0.5Pt/HY0.9	54.5	0.8	44.8	0.97
1Pt/HY0.9	48.5	0.8	50.7	1.02
2Pt/HY0.9	33.2	0.6	66.2	1.03
8Pt/HY0.9	25.7	0.6	73.7	0.96
10Pt/HY0.9	20.6	0.5	80.6	0.96

Flow circulation unit, 300 °C, 0.18 MPa of H_2, H_2/C_8H_{18} molar ratio = 16.

decreases from 8×10^{-4} mmol L^{-1} to less than detection limit (1×10^{-4} mmol L^{-1}).

In Table 4, the data on the selectivity of the *n*-octane hydroconversion depending on the activity of metallic function are shown. As the hydrogenation activity increases the selectivity shifts from the predominant cracking (82.2%) to predominant isomerization into branched octanes (80.6%), the latter representing methylheptane isomers mainly. The distribution in the C_3–C_5 cracked fraction was perfectly symmetrical with respect to the number of carbon atoms, almost equimolar amounts of C_3 and C_5 hydrocarbons were produced indicating a simple cracking of C_8H_{18} molecules by a carbenium ion mechanism. Hydrogenolysis and oligomeric cracking to C_1–C_2 and C_6–C_7 were insignificant over all the catalysts.

To test if the carbonaceous deposition (that took place to some extent over the catalysts with poor hydrogenating activity) alters the behavior of the catalysts the experiments were replicated with a pulse microreactor (PMR configuration). A diluted reaction mixture (1 vol% of *n*-octane instead of 6 vol% in previous experiments) was used to minimize deactivating effects. Under these conditions, all the catalysts including zeolites with no Pt showed quite stable operation during 5–10 repeated pulses; i.e., deactivation was not observed for a 5 to 10-pulse period. It should be noted also that in these experiments with PMR, the *n*-octane conversions over different PtHY0.9 catalysts were adjusted experimentally within the quite narrow limits of 29–31% to avoid the effect of conversion. In these tests, the concentration of *n*-octane in the reaction mixture was 0.31–0.32 mmol/L, i.e., almost the same.

Shown in Fig. 3 are the normalized reaction rates for total *n*-octane conversion, cracking, and skeletal isomerization and olefin concentration plotted as a function of k_h. Again, a similar regularity was observed: the rates of total conversion and isomerization attained constant values at $\lg k_h = 3.2$, and the cracking rate reached a maximum at this point and then decreased as k_h further increased. The increase in the selectivity to branched octanes to 93.8% was observed as k_h increased, and the selectivity to cracked products decreased from 100% over HY0.9 with no Pt to only 5.9% over 10Pt/HY0.9 (Table 5). The concentration of the olefinic cracked products decreased from 8×10^{-4} mmol L^{-1} to less than detectable limits (Fig. 3). The iso/norm ratio for the C_4–C_5 hydrocarbons was high over the catalysts with $\lg k_h \leqslant 3.2$ (2.7–2.8, Table 5), and dropped drastically to 0.6 when the hydrogenating activity further increased.

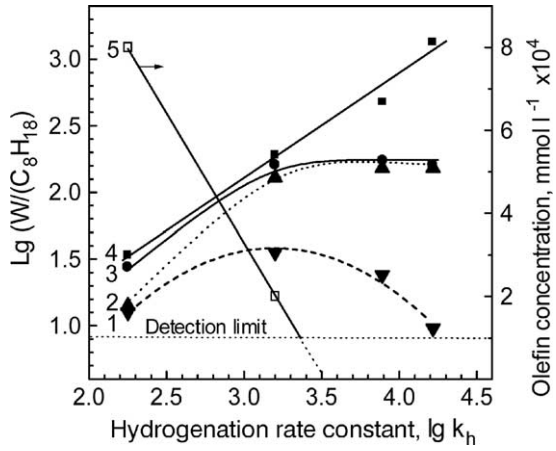

Fig. 3. The activity of Pt/HY0.9 catalysts in the *n*-octane conversion in a pulse microreactor as a function of the hydrogenating activity of the platinum component: 300 °C, 0.18 MPa, H_2 (or N_2)/C_8H_{18} molar ratio = 100. 1, Hydrocracking; 2, hydroisomerization; 3, total *n*-octane hydroconversion; 4, total *n*-octane conversion in N_2 atmosphere; 5, olefin cracked product concentration.

Quite different kinetics was observed in the same microreactor of PMR configuration when H_2 was replaced by N_2. Linear correlation between the normalized rate of *n*-octane conversion and k_h was observed over all the Pt/HY0.9 catalysts (Fig. 3). Mostly *n*-octane cracking occurred, and the selectivity to isooctanes was less than 10% over the catalyst with the strongest metallic function (10Pt/HY0.9). Significantly, the rates of cracking in H_2 and N_2 gaseous media were almost the same over the catalysts with $\lg k_h \leqslant 3.2$, but differed dramatically over Pt/HY0.9 zeolites with stronger metallic function.

3.4. n-Octane hydroconversion over HY zeolites in a flow circulation unit with CR-HR configuration depending on the reactor temperatures

Experimental data obtained are displayed in Tables 6 and 7 as a function of the temperatures in CR and HR reactors. The conversion of *n*-octane over HY zeolite alone (i.e., in the absence of 0.5% Pt/Al_2O_3 catalyst in HR reactor) at 350 °C occurred with a reasonable rate, but it decreased rapidly when operated because of deactivation due to olefin-assisted "coke" deposition. In Tables 6 and 7, the activities of HY zeolites in the tests with no Pt/Al_2O_3 catalyst referred to 15 min on stream. For example, the conversion over HY2.2 zeolite in 15 min was 36.0% (run 2).

Table 5
Selectivity of hydroconversion of *n*-octane over bifunctional Pt/HY0.9 catalysts in a pulse microreactor

Catalyst	*n*-Octane conversion (%)	W/C_8H_{18} ($L\,g^{-1}\,h^{-1}$)	Selectivity (%)			Iso/norm ratio for C_4–C_5
			Cracking	Hydrogenolysis	Hydroisomerization	
HY0.9	44.4	1.1	100.0	–	–	1.3
0.02Pt/HY0.9	31.1	27.4	48.3	–	51.6	2.8
0.2Pt/HY0.9	31.1	163.5	21.7	0.01	78.3	2.7
1Pt/HY0.9	28.9	175.0	13.3	0.1	86.2	2.0
10Pt/HY0.9	29.9	161.0	5.9	0.3	93.8	0.6

Pulse microreactor, 300 °C, 0.18 MPa, H_2/C_8H_{18} molar ratio = 100.

Table 6
Conversion of *n*-octane in the continuous-flow-circulation unit equipped with two sequential reactors as a function of the reactor temperature

Run	catalyst	Temperature (°C)		C_{olef} ($mmol\,L^{-1}$)	*n*-C_8H_{18} conversion (%)	W/C_8H_{18} ($10^{-3}\,L\,g^{-1}\,h^{-1}$)
		HY	Pt/Al_2O_3			
1	Pt/Al_2O_3	–	350	1.0×10^{-4}	1.0	0.02
2	HY2.2	350	–	8.0×10^{-2}	36.0	2.30
3	HY2.2 + Pt/Al_2O_3	350	150	4.0×10^{-4}	2.4	0.10
4	HY2.2 + Pt/Al_2O_3	350	350	5.0×10^{-3}	35.1	2.30
5	HY2.2 + Pt/Al_2O_3	200	350	1.5×10^{-3}	11.5	0.48
6	HY1.7	350	–	4.4×10^{-2}	28.6	3.85
7	HY1.7 + Pt/Al_2O_3	350	150	1.0×10^{-4}	2.3	0.25
8	HY1.7 + Pt/Al_2O_3	350	350	3.0×10^{-3}	9.7	4.40
9	HY1.7 + Pt/Al_2O_3	200	350	4.0×10^{-4}	1.8	0.69
10[a]	HY0.9	350	–	7.1×10^{-2}	67.0	27.7
11[a]	HY0.9 + Pt/Al_2O_3	350	150[b]	1.0×10^{-4}	7.7	1.8
12[a]	HY0.9 + Pt/Al_2O_3	350	350	1.0×10^{-3}	33.5	14.6
13[a]	HY0.9 + Pt/Al_2O_3	200	350	2.0×10^{-4}	17.4	4.8

Reactor CFCR of CR-HR configuration, 0.18 MPa, H_2/C_8H_{18} molar ratio = 16.
[a] H_2/C_8H_{18} molar ratio = 100.
[b] Temperature was varied from 65 to 150 °C; no effect on conversion was observed.

Table 7
Selectivity of *n*-octane conversion in the continuous-flow-circulation unit with two sequential reactors as a function of reactor temperature

Run	catalyst	Temperature (°C)		Selectivity (%)				Iso/norm ratio for C_4–C_5	C_3/C_5 ratio
		HY	Pt/Al_2O_3	C_3–C_5	C_1–C_2	C_6–C_7	*i*-C8		
1	Pt/Al_2O_3	–	350	64.4	35.6	–	–	0.05	1.0
2	HY2.2	350	–	99.4	0.6	–	–	4.0	1.0
3	HY2.2 + Pt/Al_2O_3	350	150	95.2	4.8	–	–	1.4	1.0
3	HY2.2+Pt/Al_2O_3	350	350	97.3	0.6	–	2.1	1.9	1.2
4	HY2.2+Pt/Al_2O_3	200	350	10.5	0.4	12.1	77.0	4.5	0.04
6	HY1.7	350	–	99.2	0.8	–	–	3.5	1.1
7	HY1.7 + Pt/Al_2O_3	350	150	96.8	3.2	–	–	1.4	1.1
8	HY1.7 + Pt/Al_2O_3	350	350	97.6	0.6	–	1.8	1.7	0.9
9	HY1.7 + Pt/Al_2O_3	200	350	20.4	0.6	10.7	68.3	3.9	0.1
10[a]	HY0.9	350	–	99.3	0.7	–	–	4.5	1.1
11[a]	HY0.9 + Pt/Al_2O_3	350	150[b]	98.2	1.8	–	–	1.3	1.0
12[a]	HY0.9 + Pt/Al_2O_3	350	350	95.0	0.3	–	4.7	1.5	1.2
13[a]	HY0.9 + Pt/Al_2O_3	200	350	46.7	0.8	11.5	41.0	4.9	0.6

0.18 MPa of H_2, H_2/C_8H_{18} molar ratio = 16.
[a] H_2/C_8H_{18} molar ratio = 100.
[b] Temperature was varied from 65 to 150 °C; no effect on conversion was observed.

The activity of HY zeolites was quite invariable for 10 h of operation when a 0.5% Pt/Al_2O_3 catalyst loaded in the HR reactor at a temperature of 150 °C was used, and no carbonaceous deposition was observed over zeolite, when tested for 10 h the zeolite retained its quite white color like the parent one. This contrasted with a black-colored zeolite which operated in an ordinary single reactor unit even for a short reaction period.

It can be seen from Table 6 that 0.5% Pt/Al_2O_3 catalysts at a temperature of 150 °C drastically decreased the extent

of n-octane conversion and cracking rate (compare runs 2 and 3, 6 and 7, and 10 and 11). For example, the conversion over HY2.2 zeolites decreased from 36.0% (run 2) to 2.4%. It is of importance to note that 0.5% Pt/Al_2O_3 catalysts also decreased the concentration of olefinic cracked products from 4.4–8.0 $\times 10^{-2}$ to 1.0–4.0 $\times 10^{-4}$ mmol L^{-1} at the exit of the CR reactor (compare runs 2 and 3, 6 and 7, and 10 and 11). The concentration of olefins at the entrance of the CR reactor (i.e., at the exit of HR) was below a detectable level (1.0 $\times 10^{-4}$ mmol L^{-1}). The cracked products were loosely isomerized. Iso/norm ratios for C_4–C_5 alkanes were 1.3–1.4 (iso/norm = 1.0–1.2 for butane fraction) that contrasted to 3.5–4.5 without 0.5% Pt/Al_2O_3 catalyst (Table 7). It should be noted that the variation of HR temperature from 150 °C to 65 °C showed no effect on the reaction (run 11, Table 6). Also important, the cracking rate increased significantly when the amount of Pt/Al_2O_3 catalyst in HR reactor was insufficient to provide an adequate hydrogenation of olefinic products.

A dramatic increase (by 8–23 times) in the normalized reaction rate and a high selectivity to C_3–C_5 cracked products (95.0–97.6%) was observed while increasing the temperature of HR from 150 to 350 °C (compare runs 3 and 4, 7 and 8, and 11 and 12 in Tables 6 and 7). It is of interest to note that branched octane isomers were also produced in this case with small quantities (1.8–4.7% of selectivity). The extent of isomerization of the cracked alkanes also increased compared to that obtained at 150 °C in HR (Table 7). This kinetic feature cannot be attributed to a specific activity of Pt/Al_2O_3 catalysts only, since run 1 showed a negligible n-octane conversion at 350 °C.

Upon decreasing CR temperature from 350 to 200 °C (at 350 °C in HR) the rate of n-octane conversion decreased (compare runs 4 and 5, 8 and 9, and 12 and 13), but remained significantly higher than that at 350 °C in CR and at 150 °C in HR. Major alteration of the product distribution was observed in this case (Table 7). The selectivity to branched octanes increased as high as 41.0–77.0%, and that to C_3–C_5 products decreased to 10.5–46.7%. High iso/norm ratios (3.9–4.9) and low molar C_3/C_5 ratios (much less than unity, 0.04–0.6, depending on specific activity of HY) were observed. It should be emphasized again that quite stable operation of zeolites (with different contents of Na) was observed in the reactor unit with the CR-HR configuration at different temperatures.

4. Discussion

The experiments with a circulating system with a CR-HR configuration with two separate catalytic components have made it clear that cracking and isomerization of n-octane molecules over HY zeolites at 350 °C were suppressed drastically when the Pt/Al_2O_3 catalyst realized a hydrogenating function only, and dehydrogenation reaction was not allowed to occur because of thermodynamic limitations by low temperatures (150 °C). HY zeolites behave extremely low activity under these conditions, though no carbonaceous matter is formed. The activity is quite stable, and no deactivation period is observed during a long test (up to 10 h). According to our earlier study [29–33], the very slow cracking under these conditions occurs via a monomolecular pathway. The C_3/C_5 ratio is close to unity, indicating a simple zeolite-catalyzed scission of central bonds in C_8 molecules. Most likely, monobranched C_8 species were subjected to cracking producing predominantly C_4 species with almost equimolecular amounts of n-C_4 and iso-C_4.

The rate of monomolecular cracking depends exponentially on the content of Na in HY zeolites. This strong sodium effect on the catalytic activity of HY zeolites is consistent with the data obtained by Dumesic and coworkers [23] and Engelhardt [24] for the low-temperature isobutane isomerization. H-mordenite contained 0.58 wt% Na was found [24] practically not to catalyze isobutane isomerization in the absence of olefins in the feed; however, it was able to catalyze this reaction under the same conditions with a low rate when the Na content was less than 0.1 wt% [23].

A dramatic increase in the rate of n-octane conversion with high selectivity to cracked products was observed when both dehydrogenation and hydrogenation reactions were allowed to occur over Pt/Al_2O_3 catalysts at 350 °C. In this case, octene intermediates generated in HR were transferred to a CR reactor where they cracked instaneously into C_3–C_5 hydrocarbons. Thus the evidence obtained in the reactor unit of CR-HR configuration is regarded as a distinct demonstration in favor of a classic model of nontrivial bifunctional catalysis [7]. The special tests did reveal (Table 2) the reactivity of 1-octene over HY zeolites to be by more than three orders of magnitude as reactive as that of n-octane. This made possible high rate of cracking/isomerization over bifunctional Pt/HY0.9 zeolites to be achieved despite the fact that rather a low concentration of octenes was produced because of thermodynamical limitation (equilibrium constant for n-octane dehydrogenation into different nonbranched octenes is about 1.0 $\times 10^{-2}$ at 350 °C).

The decrease of the temperature in the CR reactor from 350 to 200 °C (at 350 °C in HR) shifts the reaction pathway from predominant cracking to n-octane branching. The lower the activity of HY zeolite, the higher the selectivity to branched octanes, and the lower the selectivity to cracking. For the least active HNaY2.2 zeolite, the selectivity to isooctanes amounted thus to 77.0%, and that to cracking dropped to 10.5%. Nonsymmetrical distribution with respect to the number of carbon atoms in the cracked products was obtained in this case due to the reactions of oligomerization/β-scission that were manifested by the increased selectivity to C_6–C_7 alkanes (10.7–12.1%). The variation of the selectivity caused by temperature in CR was due to more favorable reactions of isomerization and oligomerization of intermediate octenes at low temperature as compared to cracking. However, the decrease in Na

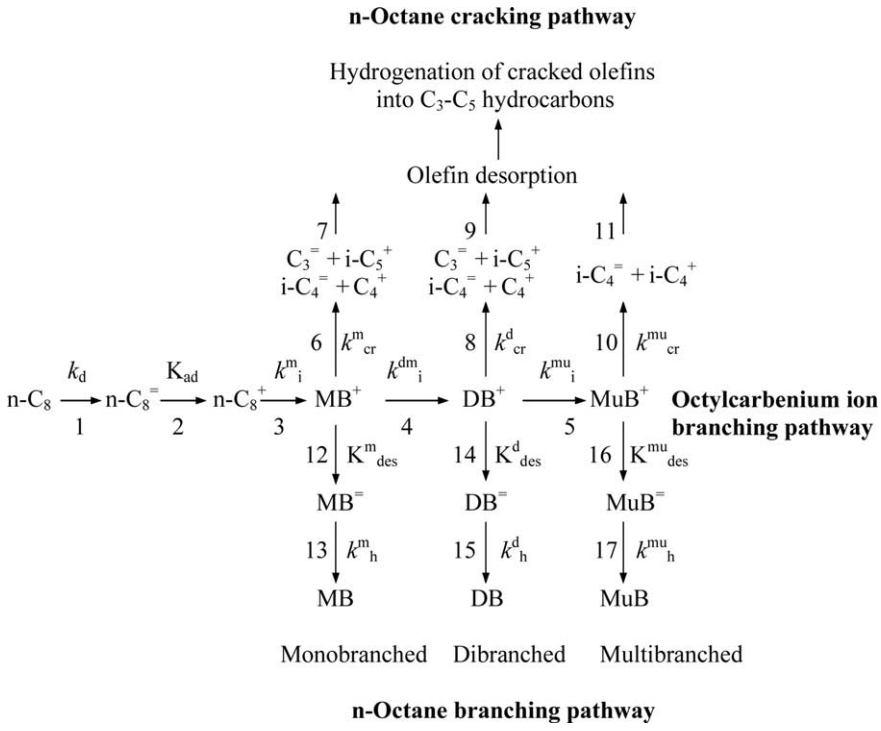

Fig. 4. Reaction network for *n*-octane hydroconversion over the Pt/HY0.9 zeolites.

content in zeolite to 0.9% made it possible to improve the selectivity to cracked products from 10.5 to 46.7% at the expense of the cracking of branched octanes apparently.

On the other hand, the increase in hydrogenating activity of the Pt component in Pt/HY0.9 catalysts improved greatly the selectivity to branched octanes. So, the balance between the acidic and metallic functions in bifunctional catalytic systems involving both separated CR + HR reactors and a single two-component Pt/HY0.9 catalyst affects dramatically the activity and selectivity to the main reaction pathways, *n*-octane cracking, and branching, occurring via a classic bifunctional mechanism.

An overall mechanistic scheme for the main reactions is depicted in Fig. 4 to better rationalize the reaction pathways depending on the relative activities of individual functions. The simplistic scheme matches the main steps of octane hydrogenation/dehydrogenation (steps 1, 13, 15, 17), formation of a secondary octyl carbenium ion by protonation of an octene intermediate (step 2), a number of successive branching rearrangements of carbenium ions (carbenium ion branching pathway) first into monobranched octylcarbenium ion MB^+ (step 3), then into dibranched octylcarbenium ion DB^+ (step 4), and finally into multibranched octylcarbenium ion MuB^+ (step 5). Branched octylcarbenium ions can desorb reversibly from the acid sites as respective branched octenes ($MB^=$, $DB^=$, $MuB^=$, steps 12, 14, and 16, respectively). The latter migrate to the metallic sites to be hydrogenated into the respective branched octanes in steps 13, 15, and 17 (*n*-octane branching pathway). Note that the reverse 15, 17, and 19 steps of dehydrogenation of branched octanes followed by adsorption of branched octenes (12, 14, and 16 reverse steps) occur simultaneously. Octylcarbenium ions listed can otherwise collapse via cracking producing C_3–C_5 cracked hydrocarbons (*n*-octane cracking pathway).

The rearrangement and scission of carbenium ions are commonly suggested [1,2,4,19,45] to be rate-determining steps, not carbenium ion formation via olefin protonation, which is considered to be rapid in zeolites. It implies octene desorption-sorption to be equilibrated with respective equilibrium desorption constants $K^{\mathrm{m}}_{\mathrm{des}}$, $K^{\mathrm{d}}_{\mathrm{des}}$, $K^{\mathrm{mu}}_{\mathrm{des}}$. Note also that according to [37], the branching of *n*-alkane, that of methyl-branched isomer, and that of dimethyl-branched isomer occur with almost identical rates. However, the cracking rate depends dramatically on the extent of branching. This is a reason why nonbranched secondary C_8^+ carbenium ion is not depicted in the cracking pathway in Fig. 4. Specific reactions of hydrogenolysis and oligomerization (i.e., formation of C_1, C_2, C_6, and C_7 alkanes) are not dispayed also in this kinetic network because of less contribution to the overall *n*-octane conversion.

With such a reaction network, one can expect that the rate of *n*-octane cracking and isomerization over bifunctional Pt/HY0.9 catalysts should be proportional to the surface concentration of octylcarbenium ions over HY0.9 zeolites. These can amount to the highest concentration level when the *n*-octane dehydrogenation rate constant k_{d} is high enough to attain equilibrium at the dehydrogenation step. The data showed (Figs. 2 and 3) the total rate of *n*-octane conversion, and the rates of skeletal isomerization and cracking to increase proportionally to the hydrogenation rate constant k_{h} (and to k_{d} consequently) until $\lg k_{\mathrm{h}}$ values were less than 3.22–3.56 ($\mathrm{L\,g^{-1}\,h^{-1}}$). This suggests that the ten-

tatively assigned *n*-octane dehydrogenation reaction is a limiting step over these catalysts. On the other hand, the rate of *n*-octane conversion did not depend on the dehydrogenating activity of catalysts with $\lg k_h \geqslant 3.56$. Hence, *n*-octane dehydrogenation attained a thermodynamical equilibrium, and octene transformations over acidic sites were the rate-determining steps. In terms of the reaction network in Fig. 4 it is clear that the transition from the Pt-limited reaction to the acid-limited one was the reason why the rate of *n*-octane conversion over bifunctional Pt/HY0.9 zeolites with $\lg k_h \leqslant 3.2$ ($L\,g^{-1}\,h^{-1}$) failed to change and increased greatly over the catalysts with more active metallic function when hydrogen was replaced by nitrogen (Fig. 3).

It is of importance to note that isooctanes produced were poorly branched over all the Pt/HY0.9 catalysts; they represented largely methylheptane isomers. In contrast, the cracked C_4–C_5 hydrocarbons produced over the catalysts with $\lg k_h \leqslant 3.89$ were highly isomerized (iso/norm ratio = 2.7–2.8) irrespectively of the hydrogenating activity. It follows from this in accordance with the evidence of the authors [1,37,45] that they were highly branched isooctenes that cracked. Poorly isomerized cracked hydrocarbons (iso/norm ratio 0.6) were produced over highly active hydrogenating 10Pt/HY0.9 catalysts. The rate of cracking culminated at $\lg k_h = 3.22$–3.89 and then significantly decreased as $\lg k_h$ further increased. Thus the cracking rate over 10Pt/HY0.9 normalized to *n*-octane concentration was lower than that over 1Pt/HY0.9 by a factor of 3. This behavior of Pt/HY0.9 catalysts with strong metallic function does not come to an agreement with the kinetically controlled network in Fig. 4 since the concentration of octene intermediates including both nonbranched n-$C_8^=$ and variously branched $MB^=$, $DB^=$, and $MuB^=$ and accordingly the concentration of respective carbenium ions could not be reduced because Pt accelerated simultaneously both forward hydrogenation steps and reverse dehydrogenation steps.

To explain the loss of the cracking ability of Pt/HY0.9 catalysts with highly active hydrogenating function, a question may be raised as to whether the acidities of Pt/HY0.9 zeolites decreased as the content of Pt increased. Actually, there are likely no reasons to believe that it is the case. All the Pt/HY0.9 samples were prepared based on the same HY0.9 zeolite. The concentration of OH groups measured by ^{1}H MAS NMR has been found [6] to be the same in the Pt/HY0.9 zeolites irrespective of the Pt content. Further, as noted, no decrease in the cracking rate in *n*-octane conversion under N_2 atmosphere was observed over the same Pt/HY0.9 zeolites as the content of Pt increased (Fig. 3). Instead, the reaction rate was proportional to the hydrogenating activity. A similar linear relationship was observed [48] when highly branched octane (2,2,4-trimethylpentane) was hydrocracked over the same Pt/HY0.9 catalysts, the rate of cracking being much higher than that of *n*-octane. This reasoning is in agreement with the evidence of other authors [11,25,37,40] who argued that the zeolites loaded with different quantities of Pt by the same procedure do not differ with the acidity. Thus, the adsorption heat and IR absorption in the range of stretching vibration of OH bonds did not change when Pt was supported on mordenite [11]. Also, it is impossible to recognize the decrease in the acidity of HY0.9 to occur due to partial pore blockage by carbonaceous matter. In fact, Pt-enriched zeolites exactly these showed quite stable operation in both flow and pulse reactors, the concentration of olefin precursors was exclusively low (less than detectable level 10^{-4} mmol/L), and carbonaceous matter was thus not formed. In summary, it follows from this reasoning that the loss of cracking ability of Pt/HY0.9 catalysts with strong metallic function cannot be referred to a decrease in the acidity of HY0.9 zeolite.

The anomaly in the cracking behavior of Pt/HY0.9 catalysts could be explained if chemical steps in the reaction network discussed were affected by diffusion steps. Diffusion and zeolite pore effects on the alkane conversion have been discussed by many authors [34–43]. The diffusion coefficient of alkanes depends significantly on the extent of branching. For example, the following sequence of diffusion coefficients for SAPO-5 was found [35]: *n*-heptane > 2-methylhexane > 3-methylhexane > 2,4-dimethylpentane > 2,3-dimethylpentane > 2,2,3-trimethylbutane. The difference in the diffusion coefficients was reflected [35] in different activities in isomerization and in the product distribution of the heptane isomers. The authors [32,39] have noted the influence of the diffusion of olefins and not the diffusion of alkanes, which is rapid compared to their chemical reactions in zeolite.

Ione [6] and Romannikov [49] have argued that the hydrogenation of linear olefins over Pt/HY zeolites at 150 °C was not affected by diffusion transfer; however, this step can become important at higher temperatures and for the bulkier branched olefins with less diffusivity. These branched olefins can be produced from the respective linear olefins inside zeolite cavities. This diffusion phenomenon can be the more pronounced the more branched octene intermediates and the larger average distance between the acidic sites and Pt sites. The production of highly isomerized cracked products over the Pt/HY0.9 zeolites with a small content of Pt is a certain indication of the occurrence of secondary reactions caused by diffusion limitations. In the Pt/HY0.9 zeolites, every metallic center is situated over the large acidic area represented by zeolite cavities. For instance, in 0.02Pt/HY zeolites, the zeolite-to-metal surface ratio is 7860, i.e., a unite of a catalytically active surface of Pt accounts for 7860 units of a zeolite surface (Table 3). Hence, on Pt-depleted zeolites, the octene intermediates contacted a large amount of acidic sites which favor multiple acid-catalyzed rearrangements into multibranched intermediates. Their sizes approach the pore size of Y zeolite, and, hence, the hydrogenation steps 13, 15, and, especially, 17 over metallic Pt can be limited by diffusion transfer. Enhanced concentration of these bulkier octene intermediates, higher than that at the equilibrium, can thus be accumulated inside the cavities.

In term of diffusion-limited hydrogenation reactions, the dependence of cracking activity and selectivity of Pt/HY0.9 catalysts with different concentrations of metallic centers can be explained analogously to that given by Alvarez et al. [37] for *n*-heptane and *n*-decane hydrocracking/isomerization over Pt/HY catalysts. The authors [37] found that the cracking over Pt/HY catalysts via β-scission of tribranched decenes which involve two tertiary carbenium ions is about 50 times faster than β-scission of dibranched isomers which involve one tertiary and one secondary carbenium ion, and 10,000 times faster than β-scission via two secondary carbenium ions. Extraordinarily high reactivity of multibranched octenes for cracking and their low diffusivity to escape zeolite cavities can be the reasons why Pt-depleted zeolite catalysts gave highly isomerized cracked products rather than respective multibranched octanes. The reaction pathway over Pt-depleted catalysts involved octylcarbenium ion branching steps 3, 4, and 5 followed by cracking into branched cracked products via step 10 predominantly. It is of significance to add that complete separation of the catalytic components to different reactors (CR-HR configuration) resulted further in a loss of the synergetic effect of acid and metallic sites that was reflected in a reduced rate of conversion and selectivity to *n*-octane branching as compared to that over PtHY0.9 catalysts (compare the data in Tables 5 and 6 for HY0.9 based catalytic systems).

In the Pt-enriched catalysts, each Pt particle accounts for smaller acidic area ($S_{\text{zeol}}/S_{\text{Pt}}$ ratio decreases to 81/102). In this case, once monobranched MB^+ octylcarbenium ions desorbed as respective olefin (step 12 with $K^{\text{m}}_{\text{des}}$ desorption equilibrium constant), the latter migrated more readily to a Pt site to be hydrogenated into the respective monobranched octane. This terminated the octylcarbenium ion branching pathway and thus shifted the cracking pathway to step 6 or 8 with the production of poorly isomerized cracked hydrocarbons with a low rate.

5. Conclusion

The application of an experimental circulating system of CR-HR configuration with two reactors loaded with separated catalytic components has made it possible to differentiate between the contribution of the olefinic cracked products and that of olefins produced from the dehydrogenation of the feed molecule to the reaction pathways. Monofunctional activity of HY zeolite in the cracking of long-chain *n*-octane molecules proved to be extremely low though no carbonaceous matter was formed and zeolites showed quite stable operation when the olefinic cracked products were removed from the reaction mixture. So, rather than improve *n*-octane cracking due to suppression of deactivation, the hydrogenation function of metallic components proved to suppress drastically the cracking. Under these conditions, a very slow zeolite-catalyzed cracking occurs via a monomolecular pathway involving the scission of predominantly central bonds most likely of monobranched C_8 species producing an equimolecular amount of *n*-butane and isobutane. The initiation of the dehydrogenation reaction over the metallic component at enhanced temperature results in a dramatic increase in the rate of zeolite-catalyzed reactions of cracking and skeletal isomerization. The evidence obtained with the reactor unit of CR-HR configuration complemented by the data over Pt/HY0.9 catalysts is regarded as a distinct demonstration in favor of a classic nontrivial model of bifunctional catalysis [7] over the catalysts based on HY zeolites.

The decrease in temperature of the CR reactor from 350 to 200 °C (at 350 °C in HR) shifts the reaction pathway from predominant cracking to *n*-octane branching. This is due to more favorable reactions of isomerization and oligomerization of intermediate octenes at low temperature as compared to cracking. The lower the activity of HY zeolite, the lower the selectivity to cracking and the higher the selectivity to branched octanes. On the other hand, the increase in the hydrogenating activity of Pt component in Pt/HY0.9 catalysts improved greatly the selectivity to branched octanes. As few as 0.2–0.5 wt% of metallic Pt in HY0.9 zeolite are required to equilibrate the reaction of *n*-octane dehydrogenation (the hydrogenation rate constant $k_{\text{h}} \geqslant 1600\ \text{L g}^{-1}\ \text{h}^{-1}$).

Complete equilibration in the hydrogenation/dehydrogenation of branched octenes may not be attained due to low diffusivity of branched octene intermediates produced inside the zeolite cavities. An enhanced concentration (higher than thermodynamically possible) of branched octenes inside the cavities makes for enchanced rate and selectivity to cracking reaction. The more the concentration of Pt sites in zeolites, the smaller the average distance between the metallic and zeolite sites, and the closer the hydrogenation/dehydrogenation reaction to the equilibration.

In closing, alkane isomerization over bifunctional catalysts in commercial units is usually thermodynamically limited. This results from the fact that the thermodynamically appropriate conditions for the reactions occurring over metallic and acidic components of bifunctional catalysts are quite different: dehydrogenation reaction needs high temperature, and isomerization needs low temperature. The application of a flow circulation unit with CR-HR configuration makes it possible to avoid the limitation. The most appropriate thermodynamical conditions for each reaction can be adjusted in this way and the exhaustive isomerization of *n*-alkanes into highly branched isomers can be attained.

References

[1] B.W. Wojciechowski, A. Corma, Catalytic Cracking; Catalysis, Chemistry, Chemistry and Kinetics, Dekker, New York, 1986.
[2] A. Corma, Chem. Rev. 95 (1995) 559.
[3] S. Kotrel, M.P. Rosynek, J.H. Lunsford, J. Catal. 182 (1999) 278.
[4] C. Stefanadis, B.C. Gates, W.O. Haag, J. Mol. Catal. 67 (1991) 363.
[5] V. Shertukde, W.K. Hall, J.-M. Dereppe, G. Marcelin, J. Catal. 139 (1993) 468.

[6] K.G. Ione, Polyfunctional Catalysis on Zeolites, Nauka, Novosibirsk, 1982.
[7] P. Weisz, Adv. Catal. 13 (1962).
[8] P. Ribeiro, C. Morcilly, M. Guisnet, J. Catal. 78 (1982) 267.
[9] P. Ribeiro, C. Morcilly, M. Guisnet, J. Catal. 78 (1982) 275.
[10] M.H. Jordao, V. Simoes, A. Montes, D. Cardoso, in: A. Corma, V.F. Melo, S. Mendioroz, J.L.G. Fierro (Eds.), Studies in Surface Sciences and Catalysis, Vol. 130, Elsevier, Amsterdam, 2000, p. 2387.
[11] R.A. Asuquo, G. Eder-Mirth, K. Seshan, J.A. Pieterse, J.A. Lercher, J. Catal. 168 (1997) 292.
[12] H.Y. Chu, M.P. Rosynek, J.H. Lunsford, J. Catal. 178 (1998) 352.
[13] W.O. Haag, R.M. Dessau, R.M. Lago, Stud. Surf. Sci. Catal. 60 (1991) 255.
[14] B.C. Gates, J.R. Katzer, G.C. Schuit, Chemistry of Catalytic Processes, McGraw–Hill, New York, 1979.
[15] J. Engelhardt, W.K. Hall, J. Catal. 125 (1990) 472.
[16] R.A. Van Santen, G. Kramer, J. Chem. Rev. 95 (1995) 637.
[17] V.B. Kazansky, M.V. Frash, R.A. van Santen, Catal. Lett. 48 (1997) 61.
[18] J.A. Dumesic, D.F. Rudd, L.M. Apancio, J.E. Rekoske, A.A. Trevmo, The Microkinetics of Heterogeneous Catalysis, Am. Chem. Society, Washington, DC, 1993.
[19] J. Engelhardt, W.K. Hall, J. Catal. 151 (1995) 1.
[20] A.G. Stepanov, K.I. Zamaraev, J.M. Thomas, Catal. Lett. 13 (1992) 407.
[21] P. Weisz, Chem. Tech. (1973) 498.
[22] K.B. Fogash, Z. Hong, J.A. Dumesic, J. Catal. 173 (1998) 519.
[23] A. Marco, M.A. Sanchez-Castillo, N. Agarwai, C. Miller, R.D. Cortright, R.J. Madont, J.A. Dumesic, J. Catal. 205 (2002) 67.
[24] J. Engelhardt, J. Catal. 164 (1996) 449.
[25] J. Engelhardt, J. Valyon, J. Catal. 181 (1999) 294.
[26] P.N. Kuznetsov, D.M. Anufriev, K.G. Ione, Kinet. Katal. 19 (1978) 536.
[27] P.N. Kuznetsov, D.M. Anufriev, K.G. Ione, Kinet. Katal. 19 (1978) 1520.
[28] D.M. Anufriev, P.N. Kuznetsov, K.G. Ione, J. Catal. 65 (1980) 221.
[29] J. Abbot, B.W. Wojciechowski, Can. Catal. 115 (1989) 1.
[30] S. Kotrel, M.P. Rosynek, J.H. Lunsford, J. Phys. Chem. B 103 (1999) 818.
[31] W.O. Haag, R.M. Dessau, in: Proceedings, 8th International Congress on Catalysis, Berlin, 1984, Vol. 2, Dechema, Frankfurt-am-Main, 1984, p. 305.
[32] B.A. Williams, W. Ji, J.T. Miller, R.Q. Snurr, H.H. Kung, Appl. Catal. 203 (2000) 179.
[33] T.F. Narbeshuber, H. Vinek, J.A. Lercher, J. Catal. 157 (1995) 388.
[34] M. Tromp, J.A. van Bokhoven, M.T. Garriga Oostenbrink, J.H. Bitter, K.P. de Jong, D.C. Koningsberger, J. Catal. 190 (2000) 209–214.
[35] M. Hochtl, A. Jentys, H. Vinek, J. Catal. 190 (2000) 419.
[36] A. Corma, V. Fornes, J. Martines-Triguero, S.B. Pergher, J. Catal. 186 (1999) 57.
[37] F. Alvarez, F.R. Ribeiro, G. Perot, C. Thomazeau, M. Guiznet, J. Catal. 162 (1996) 179.
[38] B.A. Williams, S.M. Babitz, J.T. Miller, R.Q. Snurr, H.H. Kung, Appl. Catal. A 177 (1999) 161.
[39] W.O. Haag, R.M. Lago, P.B. Weisz, J. Chem. Soc., Faraday Disc. 72 (1992) 317.
[40] G.D. Firngruber, O.P.E. Zinck-Stagno, K. Seshan, J.A. Lercher, J. Catal. 190 (2000) 374.
[41] P.D. Hopkins, J.T. Miller, B.L. Meyers, G.J. Ray, R.T. Roginski, M.A. Kuehne, H.H. Kung, Appl. Catal. A 136 (1996) 29.
[42] K.P. Moller, M. Kojima, C.T. O'Connor, Chem. Eng. J. 54 (1994) 115.
[43] J. Volter, J. Caro, M. Bulow, B. Fahlke, J. Karger, M. Hunger, Appl. Catal. 42 (1998) 15.
[44] K.G. Ione, P.N. Kuznetsov, N.V. Klyueva, G.V. Echevskii, Kinet. Katal. 18 (1977) 164.
[45] G. Yaluris, J.E. Rekoske, L.M. Aparicio, R.J. Madon, J.A. Dumesic, J. Catal. 153 (1995) 54.
[46] G. Yaluris, J.E. Rekoske, L.M. Aparicio, R.J. Madon, J.A. Dumesic, J. Catal. 153 (1995) 65.
[47] K.G. Ione, P.N. Kuznetsov, D.M. Anufriev, V.N. Romannikov, Acta Phys. Chim. 24 (1979) 153.
[48] P.N. Kuznetsov, K.G. Ione, in: J.C. Jansen, L. Moscou, M.F.M. Post (Eds.), 8th Int. Zeolite Conference, Zeolite for the Nineties, Recent Research Report, Elsevier, Amsterdam, 1989, p. 403.
[49] V.N. Romannikov, thesis, Novosibirsk, 1979.